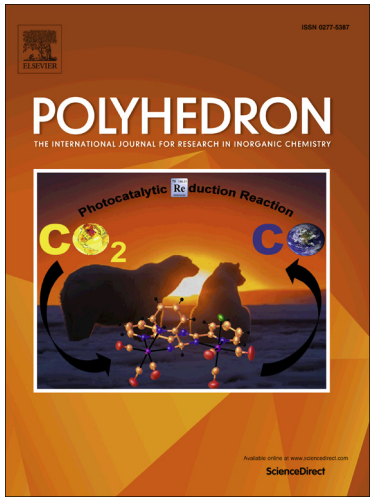

Synthesis, spectral, structural and antimicrobial studies of fluorinated porphyrins

Fasalu Rahman Kooriyaden, Subramaniam Sujatha, Chellaiah Arunkumar

PII: S0277-5387(15)00260-0
DOI: http://dx.doi.org/10.1016/j.poly.2015.05.018
Reference: POLY 11317

To appear in: *Polyhedron*

Received Date: 13 January 2015
Accepted Date: 1 May 2015

Please cite this article as: F.R. Kooriyaden, S. Sujatha, C. Arunkumar, Synthesis, spectral, structural and antimicrobial studies of fluorinated porphyrins, *Polyhedron* (2015), doi: http://dx.doi.org/10.1016/j.poly.2015.05.018

Synthesis, spectral, structural and antimicrobial studies of fluorinated porphyrins

Fasalu Rahman Kooriyaden[†], Subramaniam Sujatha[†] and Chellaiah Arunkumar[*]

Bioinorganic Materials Research Laboratory, Department of Chemistry, National Institute of Technology Calicut, Kozhikode, Kerala, India - 673 601

Abstract:

We have reported the synthesis, spectral and anti-microbial studies of 5,10,15,20-tetrakis(4′-trifluoromethylphenyl)porphyrin derivatives, MT(4′-CF_3P)Ps where M = 2H, **1**; Fe(II), **2**; Ni(II), **3**; Cu(II), **4**; Zn(II), **5** and Pt(II), **6**. The optical absorption and steady state fluorescence spectra of **1**-**6** show characteristic bands comparable with MTPPs. Compounds **1** and **3**-**5** were structurally characterized using single crystal X-ray diffraction analysis; **1** and **4** crystallized in the triclinic system, whereas **3** and **5** in the monoclinic system. The high spin nickel(II) ion in **3** is well placed at the centre of the planar porphyrin core, which is influenced by the presence of trifluoromethylphenyl groups at the periphery and two THF molecules in apex positions. The porphyrins **1** and **3**-**5** are arranged in a slip-stacked fashion involving C–H···π and C–F···$H_{(sol)}$ intermolecular close contacts for **1**, **4** and **3**, **5** respectively. The role of non-covalent interactions involving the trifluoromethylphenyl groups in the crystal packing have been analyzed and quantified using Hirshfeld surface analysis. The antimicrobial activity of the free ligand is higher compared to its metal complexes.

Keywords: Trifluoromethylphenyl porphyrin, Photophysical properties, Crystal structure analysis, Non-covalent interactions, Hirshfeld surface analysis, Antimicrobial studies.

[*] Corresponding author. Fax: 0495-2287250; E-mail address: arunkumarc@nitc.ac.in (C. Arunkumar)

[†] Equally contributed to this work.

Introduction

Porphyrinoids have been widely studied due to their spectroscopic, electrochemical and luminescent properties and their novel biological activities. Synthetic porphyrin analogues closely resemble naturally occurring tetrapyrrole macrocycles and hence they are considered to be the appropriate ligands of choice for mimicking the natural processes [1]. The introduction of suitable substituents at the peripheral positions of the porphyrin periphery provokes tunable shape, size and symmetry and are found in material [2] and therapeutic applications [3,4]. It is well known that the pharmacological properties of organic molecules can be enhanced by the incorporation of fluorine atoms which subsequently makes them more abundant in the market as effective drugs. In particular, drugs containing trifluoromethylphenyl groups, such as Prozac, Sensipar, Arava, Travatan etc, are innumerable which leads to the huge success of fluorine containing drugs in medicinal chemistry [5,6]. It is essential to analyze the various intermolecular interactions which control the structure-property relationship of the fluorinated drugs in binding to enzyme active sites. Moreover, upon fluorination, the pharmaco-kinetic properties of the molecules are pronounced which leads to better binding and hence the superior biological activity [7].

Porphyrin derivatives are excellent materials in crystal engineering [8-10] and we are interested in the design and engineering of fluorinated porphyrins in order to understand the role of close contacts involving fluorine in the crystal packing. Although fluorine substituted porphyrins and their analogues have been actively studied in the recent years [11-13], it is noted that detailed investigations on the structure and photophysical properties of fluorinated porphyrins are limited. In this line, we were stimulated to investigate the spectral and quantitative crystal structure analysis of electron deficient fluorinated metalloporphyrins containing trifluoromethylphenyl groups (Fig. 1) and the influence of such groups in the crystal packing motif of the porphyrins using Hirshfeld surface analysis [14]. Also, the antimicrobial properties of the free ligand and their metal complexes were examined with two gram-negative and two gram-positive bacterial strains, and one fungal strain.

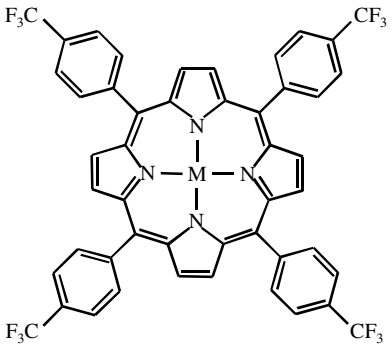

M = 2H, **1**; Fe(II), **2**; Ni(II), **3**; Cu(II), **4**; Zn(II), **5** and Pt(II), **6**

Fig. 1. Molecular structure of the porphyrins under study.

Experimental

Materials and methods

The chemicals employed for the synthesis and used in other processes were commercially available reagents of analytical grade and were used without further purification unless otherwise specified. The solvents used for the synthesis were purified using the available literature methods [15]. Optical spectra were recorded at room temperature in CH_2Cl_2 using a Systronics double beam 2202 spectrophotometer and ^1H NMR spectra were taken in a Bruker Avance III 400 MHz spectrometer. Mass spectra were recorded under ESI/HR-MS at 61,800 resolution using a Thermo Scientific Exactive mass spectrometer (Thermo Fischer Scientific, Bremen, Germany). Fluorescence spectra and quantum yield measurements were performed using a Perkin Elmer LS 55 luminescence spectrophotometer.

Synthesis of 5,10,15,20-tetrakis-(4′-trifluoromethylphenyl)porphyrin, $H_2T(4'\text{-}CF_3P)P$ and the metal complexes $MT(4'\text{-}CF_3P)P$; M = Fe(II), Ni(II), Cu(II), Zn(II) and Pt(II).

Pyrrole (0.5 mL, 7.2 mmol) and 4-(trifluoromethyl) benzaldehyde (1.0 mL, 7.2 mmol) were taken in a 500 mL two necked round bottom flask containing 350 mL of CH_2Cl_2 and the content was purged with N_2 gas for 15 min. Then, the acid catalyst $BF_3{\cdot}OEt_2$ (0.1 mL, 2.5 M) was introduced and the solution was stirred at room temperature for 1 h under an inert atmosphere, followed by the addition of 2,3-dichloro-5,6-dicyano-1,4-benzoquinone, DDQ (760 mg). The reaction mixture was further stirred for one more hour at room temperature in air, the solvent was removed by a rotary evaporator, then purification by column chromatography using

silica and hexane/chloroform as the eluent afforded the free ligand **1** in 35 % yield (550 mg). The zinc(II) and copper (II) complexes were synthesized in a chloroform/methanol mixture using the corresponding metal acetate, and the yields were obtained as 92 and 94 % respectively. The nickel(II) and iron(II) complexes were prepared in DMF using the metal chloride as the metal ion carrier, and the yield was found to be 61 and 74 % respectively. The platinum(II) complex [16] was prepared in benzonitrile using $K_2[PtCl_6]$ as the metal ion carrier and the yield was found to be 85 %. UV-Visible data of porphyrins in CH_2Cl_2, λ_{max} (log ε/M^{-1} cm^{-1}): **1**, 417 (5.81), 512 (4.59), 552 (4.21), 588 (4.20), 645 (3.99); **2**, 415 (5.86), 508 (4.87), 573 (4.33); **3**, 413 (6.26), 526 (5.31); **4**, 413 (6.10), 537 (4.86), **5**, 418 (6.28), 548 (5.03); **6**, 399 (6.20), 508 (5.17), 541 (4.67). ^{1}H NMR data for **1** in $CDCl_3$ (400 MHz): 8.81 (s, 8H, β-pyrrole-H), 8.33-8.35 (d, 8H, J = 8.00 Hz, *o*-phenyl-H), 8.04-8.06 (d, 8H, J = 8.00 Hz, *m*-phenyl-H), -2.84 (br, 2H, imino-H). ^{1}H NMR data for **3** in $CDCl_3$ (500 MHz): 8.91 (s, 8H, β-pyrrole-H), 8.34-8.36 (d, 8H, J = 8.00 Hz, *o*-phenyl-H) 8.04-8.06 (d, 8H, J = 8.00 Hz, *m*-phenyl-H). ^{1}H NMR data for **5** in $CDCl_3$ (500 MHz): 8.92 (s, 8H, β-pyrrole-H), 8.34-8.36 (d, 8H, J = 8.00 Hz, *o*-phenyl-H), 8.04-8.06 (d, 8H, J = 8.00 Hz, *m*-phenyl-H). ESI-mass data of **1**: 887.20 (calcd: 886.73).

X-ray crystal structure analysis

Suitable single crystals of the porphyrin ligand and its metal complexes were mounted on a glass capillary and the data collections were performed on a Bruker AXS Kappa Apex II CCD diffractometer with graphite monochromated Mo K_α radiation (λ = 0.71073 Å) at 298 K. The reflections with $I > 2\sigma(I)$ were employed for the structure solution and refinement. The SIR92 [17] (WINGX32) program was used for solving the structure by direct methods. Successive Fourier synthesis was employed to complete the structures after full-matrix least squares refinement on $|F|^2$ using the SHELXL97 [18] software.

Hirshfeld surface analysis

Hirshfeld surface analysis and the generation of 2D fingerprint plots were performed using *Crystal Explorer 3.1* [14].

Antimicrobial studies

The antimicrobial activity of the free ligand and its metal complexes were performed using the literature method [19] against MTCC cultures, which were obtained from the Microbial

culture collection, Chandigarh, India and are as follows: two gram-positive, *Staphylococcus aureus*, *Bacillus subtilis* and two gram-negative *Pseudomonas aeruginosa*, *Escherichia coli* bacterial strains, and the fungal strain *Candida albicans*. The ligand and its metal complexes were dissolved in dimethylsulfoxide (DMSO) to a stock solution of 250 μg/mL. The sample was loaded onto sterile discs on agar plates directly. Plates swabbed with the bacteria culture were incubated at 35-37 °C for 24 hours. At the end of the incubation period, the inhibition zones formed on the medium were evaluated in mm and studies were performed in duplicate. A solvent control test was also performed in order to study the effect of dimethylsulfoxide on the growth of the microorganism, but it showed no activity against the microbial strains. A standard antimicrobial drug (tetracycline) was also screened under similar conditions for comparison.

Results and discussion

Synthesis of the porphyrin ligand and its metal complexes

The synthesis of 5,10,15,20-tetrakis-(4′-trifluoromethylphenyl)porphyrin $H_2T(4'\text{-}CF_3P)P$, **1**, has been carried out using a modified procedure of Lindsey et al. [20] and its metal complexes $MT(4'\text{-}CF_3P)P$ (M = Fe(II), **2**; Ni(II), **3**; Cu(II), **4**; Zn(II), **5** and Pt(II), **6**) were prepared by a variant of the literature method [16,21,22]. The synthesized porphyrins were isolated, purified by column chromatography and characterized by UV-Visible and ^{1}H NMR spectroscopic methods, mass spectrometry and single crystal X-ray diffraction analysis.

*Photophysical properties of the porphyrins, **1**-**6**.*

The electronic absorption spectra of the porphyrin ligand and its metal complexes exhibited an intense Soret (B) and four/two/one visible (Q) bands, and these absorption spectral features are similar to those of the corresponding MTPPs [23]. The intensity of the Soret band is high due to an allowed $^1A_{1g} \rightarrow {}^1E_u$ transition and the peak position is in the range 413-418 nm in dichloromethane as the solvent (except for **6**, 399 nm). The overlayed UV-Visible spectra of **1**-**6** are shown in Fig. S1 and it is observed that there is a marginal red shifted absorption spectrum for the zinc(II) complex and a marginal blue shifted absorption spectra for the iron(II), nickel(II) and copper(II) complexes compared to that of the free ligand. As anticipated, the platinum(II) complex undergoes a hypsochromic shift of 18 nm with respect to the free ligand, which is attributed to the metal-to-ligand π-back bonding [24].

The fluorescent spectra of porphyrins **1**-**6** were studied in order to specify the effect of the trifluoromethyl phenyl groups on the electronic properties of the porphyrins in the excited state, using toluene as the solvent. Fig. S2 shows the fluorescence emission spectra of the various fluorinated porphyrins under study. The fluorescent spectral pattern of the free ligand **1** is similar to its tetraphenylporphyrin analogue (H_2TPP), except for the fact that the peak intensity is low in the former case, which is presumably due to the electron withdrawing nature of the trifluoromethylphenyl groups (Fig. 2). On excitation at the Soret band, all the porphyrins exhibit two well-defined emission bands in the range 598-718 nm, corresponding to the $S_1 \rightarrow S_0$ transition, and another weak emission in the range 429-456 nm, corresponding to $S_2 \rightarrow S_0$ transitions (Figure 2 and Table 1). Note, the S_2 emissions of the free base porphyrins are too weak to be detected, compared to the metalloporphyrins [25]. As reported earlier for ZnTPP, the S_2 emission is weak in intensity compared to the S_1 emission for **5** [26]. Interestingly, we observed the reverse case for the square planar nickel(II) and copper(II) complexes (**3** and **4**), whereas for the iron(II) derivative, the S_1 and S_2 peak intensities are comparable.

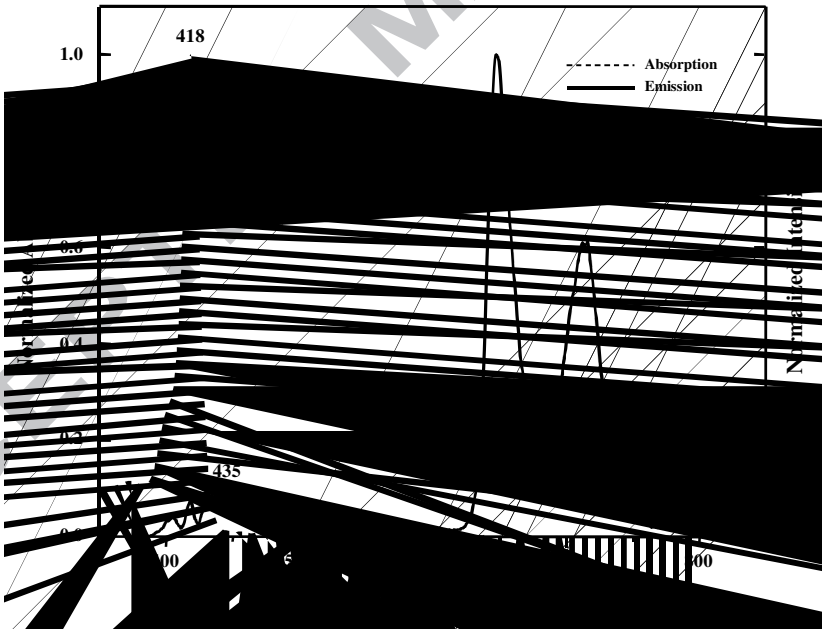

Fig. 2. Normalized emission (solid line) and absorption (dashed line) spectra of **1** in toluene at 298 K.

The Stokes shifts observed for porphyrins **1** and **5** are comparable to the corresponding values for H_2TPP and ZnTPP, which indicates that the structure of porphyrin in the excited state is similar to that of the ground state (Table 1). Thus, by changing the phenyl ring to a

trifluoromethyl phenyl ring does not result in any structural reformation in the excited state. As shown in Table 1, the S_2 emissions exhibit a larger stokes shift compared to the S_1 emissions of the [$Q_{x(0,0)}$] band [27]. The porphyrins **2**-**4** and **6** are weakly fluorescent compared to the free ligand **1** and zinc(II) derivative **5**, which may be due to the decay of the singlet excited state through internal conversion in the former cases [28]. The $S_1 \rightarrow S_0$ fluorescence quantum yields (Φ_f) of the synthesized porphyrins **1**-**6** were measured in toluene using H_2TPP as a reference [29] (Φ_f = 0.11). It is obvious from Table 1 that the incorporation of trifluoromethyl groups at the porphyrin periphery reduces the fluorescent quantum yield. Metalloporphyrins **2**-**4** and **6** show very low quantum yields compared to the free ligand **1** which indicates that the metal coordination may induce radiationless decay [30].

Table 1
Photophysical data of porphyrins **1**-**6** recorded in toluene at 300 K.

Porphyrin	**Absorption λ_{max} (nm)**	**Fluorescence[a] λ_{max} (nm)**	**Quantum Yield Φ_f (S_1-S_0)**	**Stokes Shift (nm) (S_2-S_0)**
H_2TPP	418, 516, 552, 595, 647	434, 455, 652, 716	0.110	16 (5)[b]
ZnTPP	424, 552, 588	430, 456, 598, 646	0.030	06
2H, **1**	418, 512, 552, 595, 645	435, 454, 648, 713	0.087	17 (3)[b]
Fe(II), **2**	415, 508, 573	440, 452, 601, 646	-	25
Ni(II), **3**	426, 552	433, 454, 646, 711	-	07
Cu(II), **4**	417, 541	434, 454, 651, 709	-	17
Zn(II), **5**	426, 552, 602	432, 450, 648, 708	0.012	06
Pt(II), **6**	400, 508, 539	429, 451, 650, 718	0.001	29

[a]Fluorescence spectra of the porphyrins were obtained as a function of λ_{ex} in the Soret band. [b]Stokes shifts values given in parenthesis correspond to the S_1 emission of the [$Q_{x(0,0)}$] band.

*Structural description of porphyrins, **1**, **3**, **4** and **5**.*

We successfully characterized single crystals of the porphyrins, **1**, **3**, **4** and **5**, which were grown at room temperature by the vapor diffusion method using appropriate solvents, and the data collections were also performed at room temperature (Table 2). Compounds **1** and **4**

crystallized in the triclinic system, whereas **3** and **5** crystallized in the monoclinic system. In all the compounds, the solvent molecule THF is either present in the crystalline lattice or bonded to the metal centre. The bound or unbound THF solvate molecules in all the porphyrins show the well known envelope conformation as observed in the literature [31,32]. The asymmetric unit of **1** consists of two half molecules of the porphyrin and two THF molecules, in which the porphyrin planes are found to be planar in both molecules. The ORTEP and packing diagrams of **1** are shown in Figs. 3a and 3d respectively. It is reported in the literature that the free ligand and copper(II) complex are isostructural in most porphyrins [32-34].

Table 2
Crystal structure data of the porphyrins under study: **1**, $H_2T(4'\text{-}CF_3P)P\cdot(THF)_2$; **3**, $Ni^{II}T(4'\text{-}CF_3P)P\cdot(THF)_2$; **4**, $Cu^{II}T(4'\text{-}CF_3P)P\cdot(THF)$; **5**, $Zn^{II}T(4'\text{-}CF_3P)P\cdot(THF)$.

	1	**3**	**4**	**5**
Empirical formula	$C_{56}H_{42}F_{12}N_4O_2$	$C_{56}H_{40}F_{12}N_4\ NiO_2$	$C_{52}H_{32}CuF_{12}\ N_4O$	$C_{52}H_{32}F_{12}\ N_4OZn$
fw	1030.94	1087.63	1020.36	1022.19
CCDC no.	1013690	1013689	1011088	1011087
Colour	purple	violet	brown	brown
Crystal system	triclinic	monoclinic	triclinic	monoclinic
Space group	P-1	$P2_1/n$	P-1	P21/c
a, Å	11.5014(8)	14.5791(19)	9.7136(5)	19.427(3)
b, Å	13.1179(12)	9.5303(19)	14.5452(9)	9.3940(10)
c, Å	17.3269(15)	18.351(4)	16.8870(13)	25.466(5)
α, (deg)	96.329(3)	90.0	76.608(3)	90.0
β, (deg)	92.833(3)	101.571(8)	89.617(3)	102.756(5)
γ, (deg)	108.739(3)	90.0	76.676(3)	90.0
Volume ($Å^3$)	2450.5(4)	2498.0(8)	2255.8(3)	4532.8(12)
Z	2	2	2	4
D_{calcd} (Mg/m^3)	1.397	1.446	1.502	1.498
λ, Å	0.71073	0.71073	0.71073	0.71073
T (K)	173	173	173	173
No. of unique reflections	8528	4413	7810	7986
No. of parameters refined	788	397	825	813
GOF on F^2	1.027	1.015	1.039	1.022
R_1[b]	0.0657	0.0477	0.0476	0.0465
wR_2[c]	0.1849	0.1179	0.1205	0.1129

[a] $R_1 = \Sigma||F_o|-|Fc||/\Sigma|F_o|$; $I_o > 2\sigma\ (I_o)$. [b] $wR_2 = [\Sigma\ w(F_o^2-F_c^2)^2/\Sigma w(F_o^2)^2]^{1/2}$.

Interestingly, the porphyrin core in **1** exhibits a planar skeleton whereas in **4** it is non-planar, possibly due to the presence of the 4-trifuloromethylphenyl groups and an extra THF molecule in **1** compared to **4**, which makes them non-isostructural. In compound **3**, the asymmetric unit contains half a molecule of the porphyrin and one THF molecule coordinated to

the nickel(II) centre. The ORTEP diagram of **3** consists of a nickel(II) ion which is hexa-coordinated with two THF molecules in apex positions (Fig. 3b), and the molecular crystal packing diagram is shown in Fig. 3e, formed through C–F···$H_{(sol)}$ interactions.

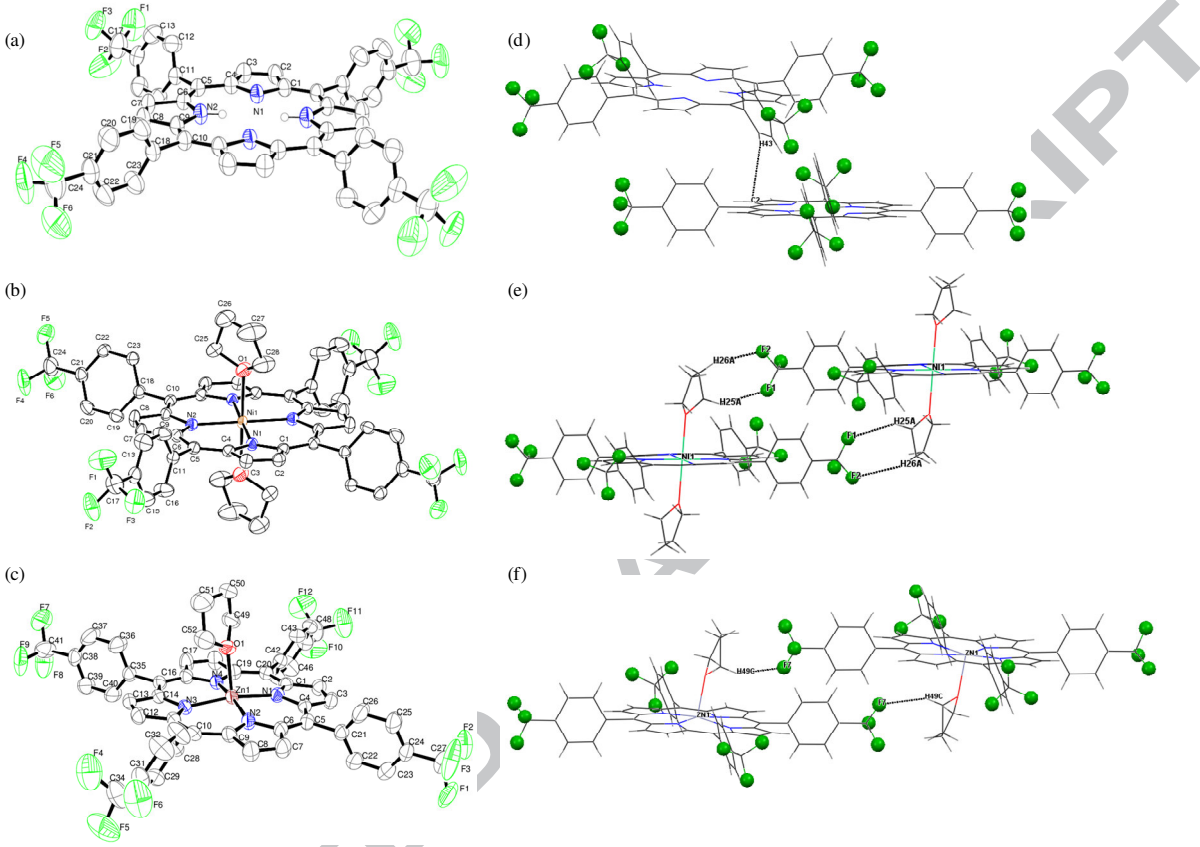

Fig. 3. ORTEP diagrams of (a) **1**, $H_2T(4'\text{-}CF_3P)P(THF)_2$ (solvent molecules and hydrogens are not shown for clarity, thermal ellipsoids are shown at the 40 % probability level); (b) **3**, $NiT(4'\text{-}CF_3P)P(THF)_2$ and (c) **5**, $ZnT(4'\text{-}CF_3P)P(THF)$. Slip-stack orientations of molecules of (d) **1**, (e) **3** and (f) **5** through C–H···π; C–F···$H_{(sol)}$ and C–F···$H_{(sol)}$ interactions respectively.

The first crystal structure of a six coordinated nickel(II) complex was reported by Schedit et al., formed by the addition of a large excess of imidazole ligands to a diamagnetic square planar nickel(II) porphyrin, which results in a high spin d^8 complex [35]. Similarly, a few more reports on high spin nickel(II) complexes of tetraphenylporphyrins bearing *β*-pyrrole electron withdrawing substituents [36-38] are available in the literature, which were prepared either by diffusing pyridine into the solution or treating the nickel(II) solution with a large excess of 1-methylimidazole at room temperature.

It is observed that the presence of either bulkier or electron withdrawing groups at the *β*-pyrrole positions makes the porphyrin core non-planar, which subsequently allows the effective installation of a high spin nickel(II) ion at the porphyrin centre [35-39]. Also, there is a lengthening of the Ni-$N_{(pyr)}$ bond distance in high spin nickel(II) porphyrins compared to that of low spin complexes, which is presumably due to the presence of one unpaired electron in the d_z^2 orbital transferred from $d_{x^2-y^2}$. Along similar lines, the elongated Ni-$N_{(pyr)}$ bond length in the planar high spin nickel(II) complex **3** is 2.051 Å, whereas the reported low spin non-planar nickel(II) centre in the MTF_4DMAP porphyrin [10] is 1.938(3) Å. This elongation of the bond length in the high spin nickel(II) complex **3** is comparable with the reported high spin complexes of planar Ni(II)-porphine (2.038(4) Å) [35] and non-planar Ni(II)-porphyrin (2.057(2) Å) [36].

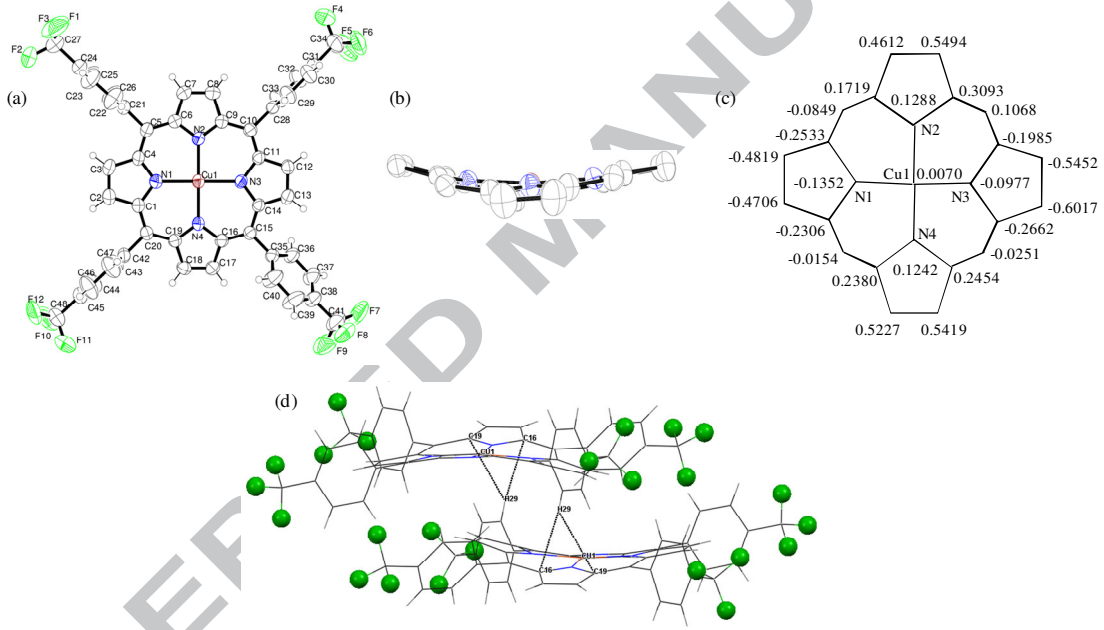

Fig. 4. ORTEP diagrams of **4**, CuT(4′-CF_3P)P (THF). (a) top view; (b) side view (the solvent molecule is not shown for clarity; thermal ellipsoids are shown at the 40 % probability level); (c) mean plane displacements of the Cu(II) ion and the core atoms shown in Å units; (d) slip-stack orientation of molecules through C–H···π interactions in **4**, CuT(4′-CF_3P)P (THF) viewed down the 'c' axis.

In addition, the N-Ni-$N_{(adj)}$ and N-Ni-$N_{(opp)}$ bond angles in **3** were found to be 90.0(10)° and 180.0(10)°, indicating the perfect planar geometry of the porphyrin core. The dihedral angles between the porphyrin mean plane and 4-trifluoromethylphenyl groups are 83.44 and 63.89°. Thus, due to the influence of the 4-trifluoromethylphenyl groups, the successful fitting of a hexa

coordinated nickel(II) ion was achieved without having *β*-pyrrole substituents at the porphyrin periphery.

The copper(II) centre in **4** is four coordinated by the inner core nitrogen atoms of the porphyrin ring, and there is an extra THF molecule present in the lattice. The porphyrin core in **4** exhibits non-planarity and the mean plane displacement of the core atoms is ± 0.3313 Å, which is less compared to that of the reported *β*-pyrrole substituted copper(II) porphyrins [40,41]. The dihedral angles between the mean plane of the porphyrin core atoms and the 4-trifluoromethylphenyl groups are 89.72, 87.60(4), 56.39 and 87.50°. The ORTEP diagrams (top and side view) and packing diagram showing the slip-stack orientation of the molecules through C–H···π interactions are also shown in Fig. 4. The non-planarity of the core is possibly due to the 4-trifluoromethylphenyl groups and solvent (THF) molecule present in the lattice.

The zinc(II) centre in **5** is five coordinated and exhibits a domed shape which is quite well known for zinc(II) complexes. The least square mean plane calculation indicates that the porphyrin plane with the metal atom is almost planar and the mean plane deviation of the core atoms is ± 0.0673 Å. However, the nitrogen atoms N3 and N4 are above the plane by 0.078(3) and 0.045(3) Å, whilst the N1, N2 and Zn atoms are below the plane by 0.107(3), 0.074(3) and 0.218(1) Å respectively [42]. The bound THF molecule is responsible for the metal being slightly pulled down from the mean plane. The 4-trifluoromethylphenyl groups make dihedral angles of 82.91(1), 86.24(1), 86.27(1) and 68.95(1)° with the porphyrin mean plane. The average Zn–N distance in **5** is 2.051(3) Å, relatively higher than the reported four coordinated ZnTPP (2.037(2) Å) and quite similar to that of five coordinated Zn(II) complexes [9,43]. The average Zn–O distance in **5** is found to be 2.23(14) Å, which is in good agreement with the values for the reported penta-coordinated Zn(II) complexes [9,43].

Like our earlier report on fluorinated porphyrins, there is an absence of either direct π–π interactions or intramolecular interactions in **1**, **3**, **4** and **5** [9,33]. The molecular crystal packing consists of a number of intermolecular interactions involving carbon, fluorine, hydrogen, oxygen and nitrogen atoms, viz. $_{(sol/ph/pyr)}$C–H···F, $_{(sol/ph/pyr)}$C–H···C$_{(sol/ph/pyr)}$, C–F···C$_{(ph/pyr)}$, $_{(ph/pyr)}$H···H$_{(sol)}$, $_{(pyr)}$C–H···O$_{(sol)}$ and F···F (Table 3). Interestingly, the H···H close contact is seen only in **4** and **5**, and the distance varies from 1.845 to 2.364 Å, which is considerably shorter compared with the previously reported fluorinated porphyrins, and this can be further supported by the Hirshfeld surface analysis discussed later.

Table 3
Distances (in Å) for the different types of interactions in the crystal packing of porphyrins **1**, **3**, **4** and **5**.

Interactions[a]	1[b]	3[b]	4[b]	5[b]
$_{(ph)}$C–H···C$_{(pyr)}$	2.727-2.895 (16)	-	2.723-2.884 (12)	2.888-2.890 (4)
$_{(sol)}$C–H···C$_{(ph)}$	-	-	2.763-2.872 (4)	-
$_{(ph)}$C–H···C$_{(sol)}$	-	-	2.658 (2)	-
$_{(pyr)}$C–H···C$_{(sol)}$	2.844-2.898 (12)	-	2.787 (2)	-
$_{(pyr)}$C–H···O$_{(sol)}$	2.566-2.573 (8)	-	-	-
$_{(ph)}$C–F···C$_{(ph)}$	3.152-3.167 (8)	-	-	-
$_{(ph)}$C–F···C$_{(pyr)}$	-	-	-	3.132 (2)
$_{(ph)}$C–F···H$_{(sol)}$	2.574 (4)	2.642-2.670 (8)	-	2.582 (2)
$_{(ph)}$C–F···H$_{(ph)}$	-	2.618 (4)	-	2.590-2.595 (4)
$_{(ph)}$C–F···H$_{(pyr)}$	-	2.669 (4)	2.664-2.670 (4)	2.641 (2)
$_{(pyr)}$H···H$_{(sol)}$	-	-	2.322 (2)	2.335 (2)
$_{(ph)}$H···H$_{(sol)}$	-	-	1.845-2.364 (6)	-
F···F	2.853 (4)	-	-	-

[a]Different types. [b]The value in parenthesis gives the number of interactions of each type per molecule.

Hirshfeld surface analysis

In order to understand and visualize the intermolecular interactions quantitatively, Hirshfeld surfaces (HSs) and 2D fingerprint plots (FPs) were generated using *Crystal Explorer 3.1* [14]. The HSs, which have been mapped over a d_{norm} range of -0.14 to 2.0 Å, are illustrated in Fig. 5. The red spots on the HSs indicate the presence of close contacts, whereas areas without close contacts are shown as blue spots.

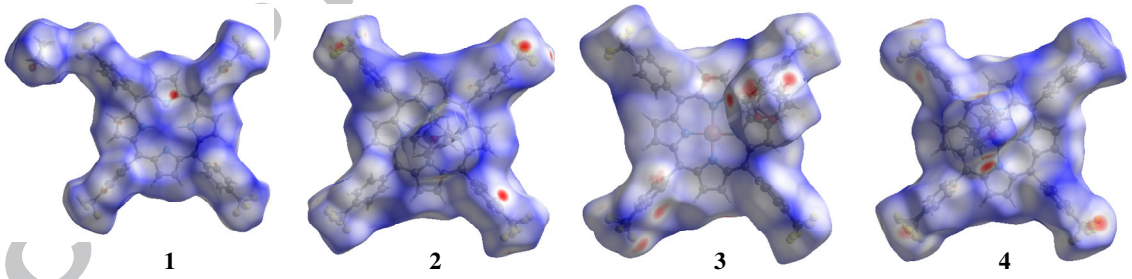

Fig. 5. Hirshfeld surfaces of porphyrins **1**, **3**, **4** and **5** with d_{norm} mapped ranging from -0.14 (blue) to 2.02 (red).

The crystal packing in porphyrins **1**, **3**, **4** and **5** is mainly controlled by the close contacts involving fluorine, i.e. F···H, which are observed as intense red spots on the HSs. The F···F contacts are also seen as large intense red spots in porphyrins **1**, **3** and **5**. The F···C contacts are observed as medium intense red spots in the free ligand **1** and its copper derivative **4**, compared

to a faint red area in the zinc derivative **5**. Apart from this, porphyrin **5** shows faint red spots for N···F close contacts. In addition to the close contacts involving fluorine, C···H contacts appear as intense and/or faint red spots in porphyrins **1** and **4**. Interestingly, unlike our recent report on the fluorinated porphyrins MT(2′,6′-DFP)P [33] and MTF$_4$DMAP [9], H···H contacts are observed as red spots in **1** and **3**, being very intense in the latter case. The shapes of the FPs of the porphyrins in **1**, **3**, **4** and **5** are incomparable, indicating that there are no isostructural pairs, which is further supported by the geometrical data discussed earlier (Table 3). The FPs of **1**, **3**, **4** and **5** feature spikes of various length and thickness, the most dominant of which is the F···H contacts in the middle region of each plot (Fig. 6). In **3** and **4**, 44 % of the intermolecular contacts are associated with F···H contacts, whereas in **1** and **5** they are associated with 36 % and 39 % of the HSs respectively.

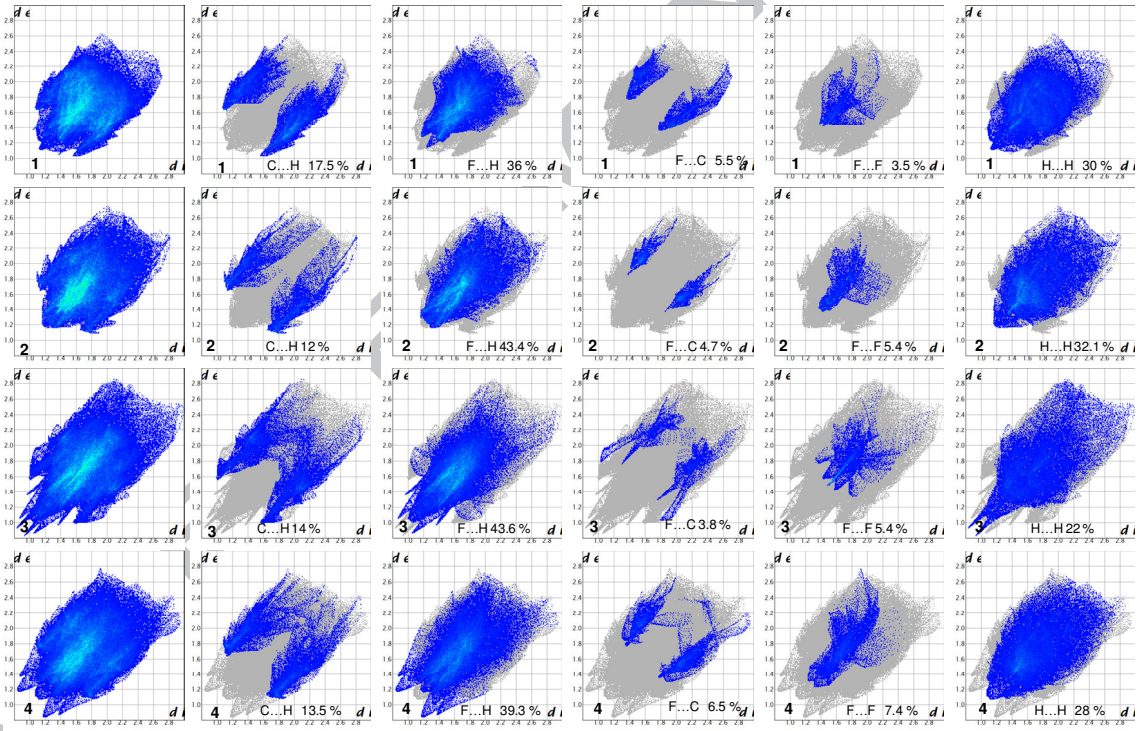

Fig. 6. Comparison of the full/decomposed FPs for the various intermolecular interactions of porphyrins **1**, **3**, **4** and **5**.

The distance (d_i + d_e) is about 2.31 to 2.44 Å for porphyrins **1**, **3**, **4** and **5**, which are significantly shorter than the corresponding sum of the van der Walls radii (2.45-2.70 Å), indicating the significant role in crystal packing [37-39]. The interactions involving fluorine

other than F···H contacts are F···F [4-5 % in **1**, **3**, **4**; 7 % in **4**] and F···C [4-7 % in **1**, **3**, **4** and **5**] with $d_i + d_e$ values in the range 2.59-2.96 and 3.14-3.20 Å respectively, which are considerably shorter than the reported values [9,33]. Also, the wing-like peripheral spikes for the C···H contacts appear at the top left and bottom right of each plot, and the percentage contributions are 18, 12, 14 and 14 % respectively for **1**, **3**, **4** and **5**. The FPs of the H···H contact are somewhat closer in nature compared to the previously reported fluorinated porphyrins, and are especially more prominent in **4**, characterized by two sharp peaks, whereas for **1**, **3** and **5** they are broader in nature. [30 % in **1**; 32 % in **3**; 22 % in **4** and 28 % in **5**]. Overall, the interactions involving fluorine are 46 % for **1** and 53-55 % for **3**–**5**, and these play a major role in directing the supramolecular architecture of the porphyrins (Fig. 7). Apart from the interactions mentioned above, the presence of other contacts, such as O···H, N···H and N···F interactions, are also observed in **1**, **3**, **4** and **5**.

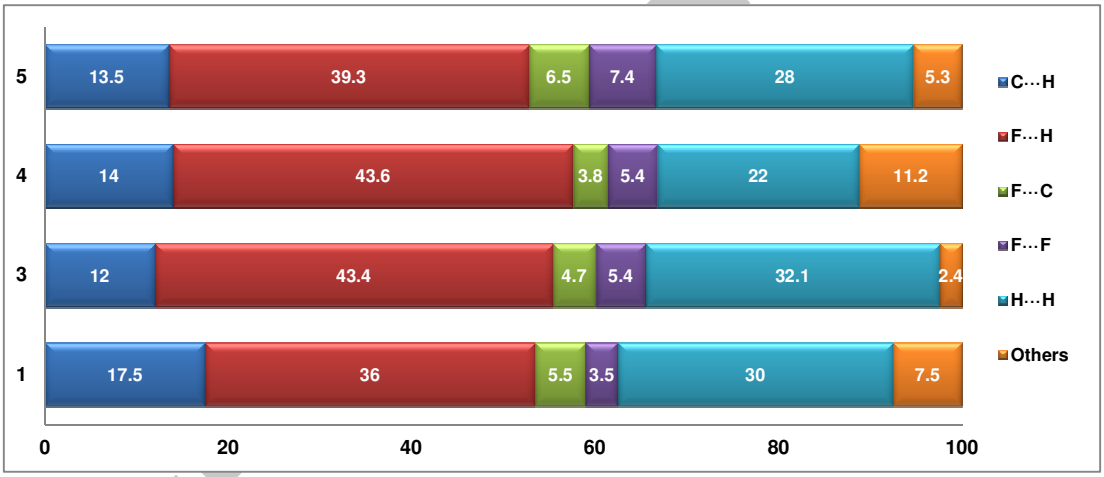

Fig. 7. Percentage contribution of non-covalent interactions in porphyrins **1**, **3**, **4** and **5** on the basis of HSs.

Antimicrobial studies of the porphyrin ligand and its metal complexes

The free ligand and its metal derivatives, **1**-**6**, were tested for their in vitro antimicrobial activity against four bacterial strains and one fungal strain by the well diffusion method at different concentrations (50, 75 and 100 µg/mL). The commercially available standard drug tetracycline was used as a control and the zones of inhibition against the control are shown in Fig. 8. All the porphyrins manifested different impacts on the different organisms. The antimicrobial activity of H_2TPP was examined under similar conditions and the results reveal that the non-fluorinated analogue shows a lesser activity compared to the fluorinated analogue

(Fig. 8). It was observed that porphyrins **1**-**6** showed the maximum zone of inhibition at the maximum concentration. At a concentration of 100 µg/mL, porphyrin **3** showed a maximum zone of inhibition of 19 mm against *E.coli*, **1** showed inhibition zones of 18 mm against *E. coli* and *B. subtilis*, **4** and **5** showed 15 and 17 mm of inhibition zones respectively against *E.coli*. At 75 µg/mL concentration, a maximum zone of inhibition of 16 mm was recorded for **3**, followed by 15 and 14 mm for **6** and **4** respectively against *E. coli*. At 50 µg/mL of concentration, a maximum zone of inhibition was recorded on **3** against *E. coli*, followed by **6** and **1** against *B. subtilis*. There was no activity observed for compounds **4** and **6** against *B. subtilis* or for **2** and **3** against *P.aeruginosa*. In the case of the fungal strain *C. albicans*, the maximum activity was found for porphyrin **2**, followed by **3** and no activity was found for **5** (Fig. 8). Among all the compounds, the antimicrobial activity of the free base porphyrin showed the maximum zone of inhibition towards all five microorganisms and the order of activity is as follows: **1** > **3** > **2** > **4** > **5** > **6**. Overall, the structure of the cell membrane may be altered by the porphyrin molecules due to their affinity to biological organisms and this could be the reason for the biological activity [44].

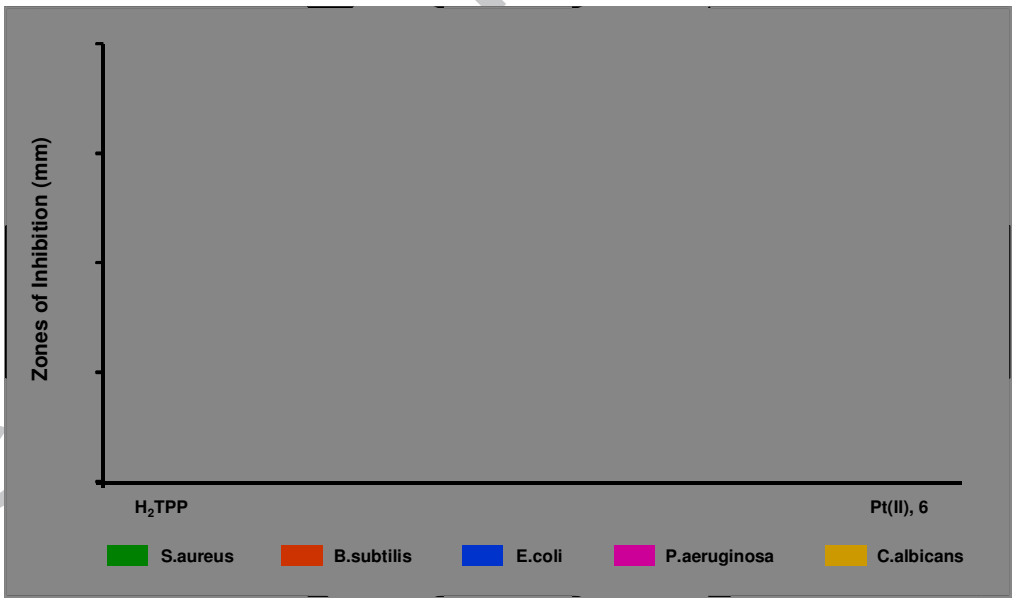

Fig. 8. Comparison of the antimicrobial activities of the studied porphyrins **1**-**6** along with H_2TPP.

Conclusions

In conclusion, the synthesis and photophysical properties of a fluorinated porphyrin and its metal derivatives were explored. Steady state fluorescence spectra of the porphyrins **1**-**6** exhibit dual emission bands originating from the $S_2 \rightarrow S_0$ and $S_1 \rightarrow S_0$ states. The fluorescent quantum yield is higher for the free ligand and the zinc(II) derivative compared to the other metal derivatives. Compounds **1** and **3**-**5** have been structurally characterised using experimental crystallographic studies along with computational analysis. The geometrical and Hirshfeld surface analyses indicate that the free ligand **1** and copper(II) complex **4** are non-isostructural, which may be possibly due to the influence of the trifluoromethylphenyl groups and the difference in the solvated THF molecule(s). The effective installation of a six coordinated nickel(II) ion with two THF molecules present at the apex positions in the planar porphyrin core was successfully achieved. Compounds **3** and **5** showed several F···H interactions which allow the molecules to orient in a slip-stack fashion, leading to 2D networks, whereas in **1** and **4** contain C···H interactions. From the FPs, it can be concluded that the back bone of the net supramolecular arrangements are dictated by close contacts involving fluorine [46 % for **1** and 53-55 % for **3**-**5**]. The antibacterial and antifungal activities of all the synthesised porphyrins were examined and the results show that the free ligand is highly effective compared to its metal derivatives; also their inhibitory capabilities are concentration dependent.

Acknowledgements

The authors, SS (SR/WOS-A/CS-146/2011) and CA (SR/FT/CS-25/2011, SB/EMEQ-016/2013) thank DST, New Delhi for financial support. We also thank Dr. Shibu M Eappen, STIC, CUSAT, Kochi and Dr. Babu Varghese, SAIF, IIT Madras for the single crystal data collection and structure solution, refinement respectively.

Appendix A. Supplementary Data

CCDC 1013690, 1013689, 1011088 and 1011087 contain the supplementary crystallographic data for porphyrins **1**, **3**, **4** and **5**. These data can be obtained free of charge via http://www.ccdc.cam.ac.uk/conts/retrieving.html, or from the Cambridge Crystallographic Data

Centre, 12 Union Road, Cambridge, CB2 1EZ, UK; Fax: + 44 123 336 033; or e-mail: deposit@ccdc.cam.ac.uk.

References

[1] K.M. Kadish, K.M. Smith, R. Guilard, (Ed.), *The Porphyrin Handbook*, Academic Press, San Diego, CA, 2000, vol. 1-20.

[2] (a) J.-H. Chou, M.E. Kosal, H.S. Nalwa, N.A. Rakow, K.S. Suslick in *The Porphyrin Handbook*, Academic Press, San Diego, CA, 2000, vol. 6, 43-131;
(b) Y. Feng, J. Cheng, L. Zhou, X. Zhou, H. Xiang, Analyst, 137 (2012) 4885-4901.

[3] T. Goslinski, J. Piskorz, J. Photochem. Photobiol. C: Photochem. Rev. 12 (2011) 304-321.

[4] S. Rani-Beeram, K. Meyer, A. McCrate, Y. Hong, M. Nielsen, S. Swavey, Inorg. Chem. 47 (2008) 11278-11283 and references therein.

[5] I. Ojima (Ed.), *Fluorine in Medicinal Chemistry and Chemical Biology*; Wiley-Blackwell: UK, 2009.

[6] K.L. Kirk, J. Fluor. Chem. 127 (2006) 1013-1029.

[7] (a) J.A. Olsen, D.W. Banner, P. Seiler, B. Wagner, T. Tschopp, U. Obst-Sander, M. Kansy, K. Muller, F. Diederich, ChemBioChem. 5 (2004) 666-675;
(b) B.E. Smart, J. Fluor. Chem. 109 (2001) 3-11.

[8] K.M. Barkigia, P. Battioni, V. Riou, D. Mansuy, J. Fajer, Chem. Commun. (2002) 956–957.

[9] R. Soman, S. Sujatha, S. De, V.C. Rojisha, P. Parameswaran, B. Varghese, C. Arunkumar, Eur. J. Inorg. Chem. (2014) 2653-2662.

[10] I. Goldberg, CrystEngComm. 4 (2002) 109-116.

[11] S.G. DiMagno, J.C. Biffinger, H. Sun, *Fluorinated Porphyrins and Corroles: Synthesis, Electrochemistry, and Applications, Fluorine in Heterocyclic Chemistry,* Vol. 1, 2014, pp 589-620.

[12] P.A. Stuzhin, *Fluorinated Phthalocyanines and Their Analogues, Fluorine in Heterocyclic Chemistry,* Volume 1, 2014, pp 621-681.

[13] S.K. Pandey, A.L. Gryshuk, A. Graham, K. Ohkubo, S. Fukuzumi, M.P. Dobhal, G. Zheng, Z. Ou, R. Zhan, K.M. Kadish, A. Oseroff, S. Ramaprasad, R. K. Pandey, Tetrahedron 59 (2003) 10059-10073.

[14] S.K. Wolff, D.J. Grimwood, J.J. McKinnon, M.J. Turner, D. Jayatilaka, M.A. Spackman, Crystal Explorer 3.1 (2013), University of Western Australia, Crawley, Western Australia, 2005-2013; http://hirshfeldsurface.net/CrystalExplorer.

[15] D.D. Perrin, W.L.F. Armarego, *Purification of Organic Solvents*, Pergamon Press, Oxford, 1988.

[16] R.C. Kwong, S. Sibley, T. Dubovoy, M. Baldo, S.R. Forrest, M.E. Thompson, Chem. Mater. 11 (1999) 3709-3713.

[17] A.G. Altomare, G. Cascarano, C. Giacovazzo, A. Gualardi, J. Appl. Crystallogr. 26 (1993) 343-350.

[18] G.M. Sheldrick, SHELXL97; University of Göttingen: Göttingen, Germany, 1997.

[19] D. Greenwood, R. Snack, J. Peurtherer, *Medical Microbiology, A Guide to Microbial Infections, Pathogenesis, Immunity, Laboratory Diagnosis and Control*, 15th Ed, 1997.

[20] J.S. Lindsey, I.C. Schreiman, H.C. Hsu, P.C. Kearney, A.M. Marguerettaz, J. Org. Chem. 52 (1987), 827-836.

[21] P. Bhyrappa, V. Krishnan, Inorg. Chem. 30 (1991) 239-245.

[22] (a) P. Bhyrappa, S.R. Wilson, K.S. Suslick, J. Am. Chem. Soc. 119 (1997) 8492-8502;
(b) W. Wu, W. Wu, S. Ji, H. Guo, X. Wang, J. Zhao, Dyes Pigm. 89 (2011) 199-211;
(c) X. Wang, X. Chen, Z. Xie, X. Wang, Angew. Chem. 47 (2008) 7450-7453.

[23] M. Meot-Ner, A.D. Adler, J. Am. Chem. Soc. 97 (1975) 5107-5111.

[24] L.M. Mink, M.L. Neitzel, L.M. Bellomy, R.E. Falvo, R.K. Boggess, B.T. Trainum, P. Yeaman, Polyhedron, 16 (1997) 2809-2817.

[25] M. Gouterman, P.M. Rentzepis, *Porphyrins: Excited States and Dynamics (ACS Symposium Series)* 1987.

[26] S. Tobita, Y. Kaizu, Y. Kobayashi, I. Tanaka, J. Chem. Phys. 81 (1984) 2962-2969.

[27] (a) N. Venkatramaiah, B. Ramakrishna, A. R. Kumar, N. Veeraiah, R. Venkatesan, J. Alloys Compd. 513 (2012) 318-323.
(b) K.P. Chandra Shekar, B. Mishra, A. Kumar, S. Phukan, S. Mitra, D. Kumar, J. Porphyrins Phthalocyanines 14 (2010) 1034-1039.

[28] I. Gupta, M. Ravikanth, J. Chem. Sci. 117 (2005) 161-166.

[29] (a) O. Ohno, Y. Kaizu, H. Kobayashi, J. Chem. Phys. 82 (1985) 1779-1787;
(b) P.G. Seybold, M. Gouterman, J. Mol. Spectrosc. 31 (1969) 1-13.
(c) M.M. Kruk, A.S. Starukhin, W. Maes, Macroheterocyles 4 (2011) 69-79.
(d) J. Karolczak, D. Kowalska, A. Lukaszewicz, A. Maciejewski, R.P. Steer J. Phys. Chem. A 108 (2004) 4570-4575.

[30] T. Zoltan, F. Vargas, V. Lopez, V. Chavez, C. Rivas, A.H. Ramirez, Spectrochim. Acta Part A Mol. Biomol. Spectrosc. 135 (2015) 747-756.

[31] C.A. Reed, T. Mashiko, W.R. Scheidt, K. Spartalian, G. Lang, J. Am. Chem. Soc. 102 (1980) 2302-2306.

[32] C.K. Schauer, O.P. Anderson, S.S. Eaton, G.R. Eaton, Inorg. Chem. 24 (1985) 4082-4086.

[33] R. Soman, S. Sujatha, C. Arunkumar, J. Fluor. Chem. 163 (2014) 16-22.

[34] E.R. Birnbaum, J.A. Hodge, M.W. Grinstaff, W.P. Schaefer, L. Henling, J.A. Labinger, J.E. Bercaw, H.B. Gray, Inorg. Chem. 34 (1995) 3625-3632.

[35] J.F. Kirner, J. Garofalo Jr, W.R. Scheidt, Inorg. Nucl. Chem. Lett. 11 (1975) 107-112.

[36] H. Duval, V. Bulach, J. Fischer, R. Weiss, Inorg. Chem. 38 (1999) 5495-5501.

[37] P. Bhyrappa, M. Sankar, B. Varghese, Inorg. Chem. 45 (2006) 4136-4149.

[38] M.W. Renner, K.M. Barkigia, D. Melamed, K.M. Smith, J. Fajer, Inorg. Chem. 35 (1996) 5120-5121.

[39] A.L. Balch, M.M. Olmstead, S.L. Phillips, Inorg. Chem. 32 (1993) 3931-3936.

[40] P. Bhyrappa, C. Arunkumar, J. Chem. Sci. 122 (2010) 233-238.

[41] P. Bhyrappa, C. Arunkumar, B. Varghese, D.S. Sankara Rao, S.K. Prasad, J. Porphyrins Phthalocyanines 12 (2008) 54-64.

[42] W.R. Scheidt, in *The Porphyrin Handbook,* Academic Press, New York, 2000, vol. 3, 49-112.

[43] P. Bhyrappa, C. Arunkumar, J.J. Vittal, J. Chem. Sci. 117 (2005) 139-143.

[44] A. Hou, Z. Xue, Y. Liu, S. Qu, W. Wang, Chem. Biodivers. 4 (2007) 1492-1500.

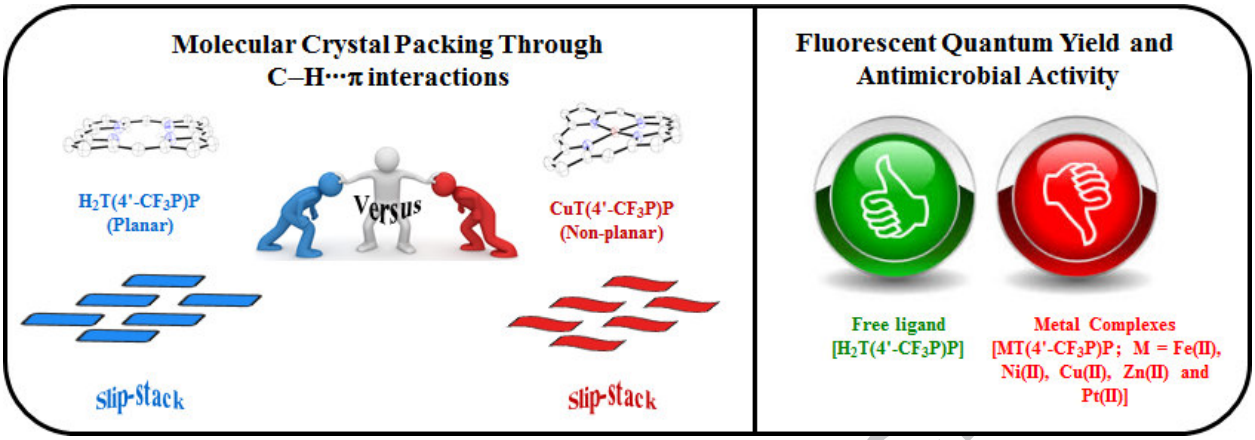

Graphical abstract

Effect of trifluoromethylphenyl groups:

The free ligand and the copper(II) complex of MT(4′-CF_3P)Ps are non-isostructural, being influenced by intermolecular interactions involving trifluoromethylphenyl groups and solvent (THF) molecules. It is evident from Hirshfeld surface analysis that the arrangements of the supramolecular networks are dictated by the close contacts involving fluorine (F···H) and other C···H and H···H contacts.